

000 001 002 003 SELF-IMPROVING MODEL STEERING 004 005 006 007

008 **Anonymous authors**
009
010
011
012
013
014
015
016
017
018
019
020
021
022
023
024

Paper under double-blind review
025
026
027
028
029
030
031
032
033
034
035
036
037
038
039
040
041
042
043
044
045
046
047
048
049
050
051
052
053

ABSTRACT

Model steering represents a powerful technique that dynamically aligns large language models (LLMs) with human preferences during inference. However, conventional model-steering methods rely heavily on externally annotated data, not only limiting their adaptability to varying contexts but also tethering their effectiveness to annotation quality. In this paper, we present SIMS, the first self-improving model-steering framework that operates without relying on external supervision. At its core, SIMS autonomously generates and refines contrastive samples through iterative self-improvement cycles, enabling adaptive, context-specific steering. Additionally, SIMS employs novel strategies, including prompt ranking and contrast sampling, to further enhance steering efficacy. Extensive evaluation across diverse LLMs and benchmarks demonstrates that SIMS substantially outperforms existing methods in steering effectiveness and adaptability, highlighting self-improving model steering as a promising direction for future research on inference-time LLM alignment. The code for replicating SIMS is available at <https://anonymous.4open.science/r/SIMS/>

1 INTRODUCTION

Model steering (Panickssery et al., 2023; Li et al., 2023; Qiu et al., 2024) represents a compelling alternative to pre- and post-training alignment methods for large language models (LLMs) (Ouyang et al., 2022; Lee et al., 2024b). By modifying latent activations with pre-computed steering vectors on the fly, it enables alignment without expensive retraining. A variety of approaches have been proposed to compute the steering vectors, ranging from linear transformations and projections (Panickssery et al., 2023; Li et al., 2023) to subspace learning and optimization techniques (Qiu et al., 2024; Pham & Nguyen, 2024; Zhang et al., 2024; Cao et al., 2024). However, as illustrated in Figure 1 (a), most existing methods rely heavily on labeled alignment datasets to optimize steering vectors. This dependence assumes complete prior knowledge of what constitutes good versus bad examples through pre-existing datasets, an assumption with two major limitations. First, it demands access to diverse data sources, including outputs from different LLMs with varying architectures and sizes, or extensive human annotations. Second, it requires high-quality labels that accurately capture response alignment with specific objectives. Together, these requirements significantly limit the practical applicability of model steering.

In this paper, we explore whether we can derive high-quality steering vectors using only the data from the LLM itself. We present SIMS,¹ a model-steering framework that enables model alignment through iterative refinement of the model’s own responses. As illustrated in Figure 1 (b), SIMS distinguishes itself from conventional methods through two fundamental innovations. *i) Self-play steering* – SIMS eliminates dependency on external responses and their corresponding labels by leveraging self-generated samples to derive steering directions. This paradigm shift enhances adaptability to varying contexts and data distributions. *ii) Iterative self-improvement* – through cycles of evaluation and

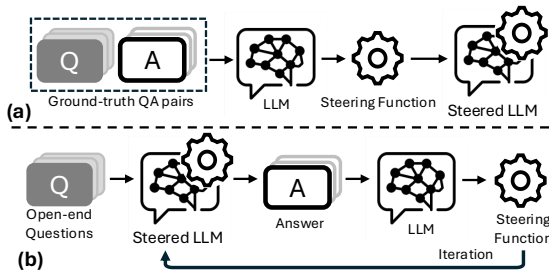


Figure 1: Comparison of (a) conventional and (b) self-improving model steering.

¹SIMS: Self-Improving Model Steering.

054 regeneration, SIMS continuously refines steering directions to more effectively differentiate desirable
 055 and undesirable behaviors, leading to consistent performance gains across iterations. Additionally,
 056 we introduce two variants to further enhance steering efficacy: *i*) prompt ranking (SIMS-PR), which
 057 leverages the model’s own judgment to generate preference signals, eliminating the need for external
 058 oracles and enabling fully autonomous self-improvement; and *ii*) contrast sampling (SIMS-CS), which
 059 maintains a response bank to select the most informative question-response pairs across iterations,
 060 thereby improving sampling efficiency.

061 Through extensive evaluation across diverse LLMs and benchmarks, we show that SIMS effectively
 062 steers LLMs towards desirable behaviors, outperforming or matching existing model-steering methods
 063 that rely on externally annotated data. For instance, SIMS improves the length-controlled WinRate
 064 of `11ama3-8b` on Alpaca-Eval (Dubois et al., 2025) from 2.86 to 11.89 in just one iteration. Our
 065 ablation study further reveals that SIMS steadily enhances steering effectiveness across iterations,
 066 while SIMS-PR and SIMS-CS substantially improve steering efficiency. For example, SIMS increases
 067 the Arena-Hard (Li et al., 2024) score sharply from 15.3 to 33.4 from the first iteration to the third
 068 iteration. The findings highlight self-improving model steering as a promising direction for future
 069 research on inference-time preference optimization.

070 Our contributions can be summarized as follows.

- 072 • We introduce SIMS, a novel self-improving model-steering framework that iteratively refines
 073 steering directions through self-improvement cycles, enabling adaptive, context-specific steering.
- 074 • We further implement two variants of SIMS, namely SIMS-PR and SIMS-CS. SIMS-PR leverages
 075 the model’s own judgment to generate preference signals, while SIMS-CS selects informative
 076 samples for refining steering directions.
- 077 • We conduct an extensive evaluation to validate that SIMS effectively guides LLMs towards desir-
 078 able behaviors, consistently outperforming or matching existing methods that require externally
 079 annotated data.

080 2 RELATED WORK

083 **Model Steering.** Unlike pre/post-training alignment (Ouyang et al., 2022; Lee et al., 2024b), model
 084 steering modifies latent activations at inference time (Turner et al., 2023; Liu et al., 2023; Zou
 085 et al., 2023; Wu et al., 2024c; Chalnev et al., 2024; Lee et al., 2024a; He et al., 2024; Fang et al.,
 086 2024; Rodriguez et al., 2024; Wang et al., 2024; Liu et al., 2024a; Cao et al., 2024). Methods differ
 087 by how steering vectors are obtained. Linear approaches (Turner et al., 2023; Panickssery et al.,
 088 2023; Li et al., 2023) derive vectors from activations: ActADD (Turner et al., 2023) uses activation
 089 differences elicited by opposing prompts (e.g., truthful versus deceptive), and CAA (Panickssery
 090 et al., 2023) averages differences between paired positive/negative prompts. Nonlinear interven-
 091 tions (Qiu et al., 2024; Zhang et al., 2024; Pham & Nguyen, 2024) act in learned subspaces; e.g.,
 092 HPR (Pham & Nguyen, 2024) learns global separating hyperplanes and rotations to reflect and rotate
 093 activations toward desirable behavior. However, most methods rely on externally annotated data (e.g.,
 094 question-answer pairs), limiting adaptability and tying effectiveness to annotation quality.

095 **Preference optimization.** Reinforcement learning from human feedback (RLHF) has emerged as
 096 a prominent approach for learning human preferences (Ouyang et al., 2022; Lee et al., 2024b). RLHF
 097 first trains a reward model on preference data using established frameworks (e.g., the Bradley-Terry
 098 model (Huang et al., 2004)), and applies RL algorithms (e.g., PPO (Schulman et al., 2017)) to optimize
 099 LLMs with respect to the reward model. Recent work (Rafailov et al., 2023; Zhao et al., 2023) shows
 100 the feasibility of bypassing the explicit reward modeling and directly solving the underlying RL
 101 problem. Further, SRSO (Liu et al., 2024b) unifies the losses of DPO (Rafailov et al., 2023) and
 102 SLiC (Zhao et al., 2023), offering an improved estimate of the optimal policy. This work extends
 103 previous research on preference optimization into challenging scenarios where externally annotated
 104 data is unavailable or impractical to obtain, addressing a critical gap in current work.

105 **LLM Self-Improvement.** Self-improvement, in which models generate, judge, and refine their
 106 own outputs, can enhance alignment, instruction following, and preference modeling while reducing
 107 annotation effort and exposure to harmful content (Chen et al., 2025; Dong et al., 2024b; Song
 108 et al., 2024; Subramaniam et al., 2025; Choi et al., 2024; Wu et al., 2024a; Peng et al., 2024; Wan
 109 et al., 2025). Approaches include synthetic preference generation (Dong et al., 2024b; Lee et al.,

2024b), tree-search refinement (Cheng et al., 2024; Light et al., 2023), Nash-equilibrium-based optimization (Wu et al., 2024b), execution-guided verification (Dong et al., 2024a), and iterative self-evolved reward modeling (Huang et al., 2024), differing mainly in feedback mechanism and granularity (internal judgment, strategic refinement, external execution validation). To our best knowledge, this work represents the first exploration of this paradigm for model steering.

3 PRELIMINARIES

3.1 MODEL STEERING

Let \mathcal{M} denote an L -layer, Transformer-based LLM and x be a tokenized prompt. The embedding matrix W_E maps tokens to the initial hidden state $h_0 = W_E(x)$. For each layer $l \in [L]$, we apply multi-head attention (MHA) followed by a position-wise feed-forward network (FFN), each with a residual connection:²

$$h'_l = h_{l-1} + \text{MHA}_l(h_{l-1}), \quad h_l = h'_l + \text{FFN}_l(h'_l). \quad (1)$$

The model’s logits are obtained via $\mathcal{M}(x) = W_U(h_L)$, where W_U is the un-embedding matrix.

During inference, we inject steering functions f_l and f'_l into the residual stream:

$$\tilde{h}'_l = \tilde{h}_{l-1} + \text{MHA}_l(f_l(\tilde{h}_{l-1})), \quad \tilde{h}_l = \tilde{h}'_l + \text{FFN}_l(f'_l(\tilde{h}'_l)), \quad (2)$$

where f_l (respectively f'_l) operates immediately before the attention (respectively FFN) while the residual addition preserves the original signal. The steered model then produces $\tilde{\mathcal{M}}(x) = W_U(\tilde{h}_L)$.

Given a dataset $\mathcal{D} = \{(x_i, y_i^+, y_i^-)\}_{i=1}^N$, where y_i^+ (desired) and y_i^- (undesired) exhibit opposite attributes, we form positive and negative samples (x_i, y_i^+) and (x_i, y_i^-) , respectively. Passing these examples through \mathcal{M} yields paired hidden activation sets:

$$\mathcal{H}_l^+ = \{(h_{l,i}^+, h'_{l,i}^+)\}_i, \quad \mathcal{H}_l^- = \{(h_{l,i}^-, h'_{l,i}^-)\}_i. \quad (3)$$

Existing model-steering methods learn f_l and f'_l by exploiting the discrepancy between \mathcal{H}_l^+ and \mathcal{H}_l^- using contrastive or other representation-learning objectives (details in §2). We refer to these methods as *steering-function learners* in the following.

3.2 SELF-IMPROVEMENT LEARNING

We formalize the self-improvement optimization as follow. Given an LLM \mathcal{M} , we prompt \mathcal{M} with input x and obtain two responses y and y' .

The self-improvement learning aims to optimize the alignment of \mathcal{M} to human preferences. This process is typically done by reinforcement learning, which \mathcal{M} represents the initial policy π_0 . A preference oracle \mathcal{O} , obtained from human feedback, is introduced in the learning process. Given the input x and two responses y and y' , The oracle \mathcal{O} will provide preference feedback $o(y \succ y'|x) \in \{0, 1\}$ indicating whether y is preferred over y' . We denote $\mathbb{P}(y \succ y'|x) = \mathbb{E}[o(y \succ y'|x)]$ as the probability of y ‘winning the duel’ over y' . In addition, we define the winning probability of y against a distribution of responses from policy π as

$$\mathbb{P}(y \succ \pi|x) = \mathbb{E}_{y' \sim \pi(\cdot|x)} [\mathbb{P}(y \succ y'|x)]. \quad (4)$$

The self-improvement learning takes an iterative process to update the policy π_t , where t denotes the iteration number. For every iteration t , π_t is optimized based on the objective function as:

$$\pi_{t+1} = \arg \max_{\pi} \mathbb{E}_{x \sim \mathcal{D}} (\mathbb{E}_{y \sim \pi(\cdot|x)} \mathbb{P}(y \succ \pi_t|x)). \quad (5)$$

However, the above equation is hard to optimized directly through gradient. Reference probability $\mathbb{P}(y \succ \cdot)$ is typically non-smooth and lead to high-variance. To overcome this shortcomings, many works adopt KL-regularized, max-entropy RL objective as follows

$$\pi_{t+1} = \arg \min_{\pi} \mathbb{E}_{y \sim \pi_t(\cdot|x)} \left[\left(\log \frac{\pi(y|x)}{\pi_t(y|x)} - (\eta \mathbb{P}(y \succ \pi_t|x) - \log Z_{\pi_t}(x)) \right)^2 \right], \quad (6)$$

²Layer normalization and projection matrices are omitted for clarity.

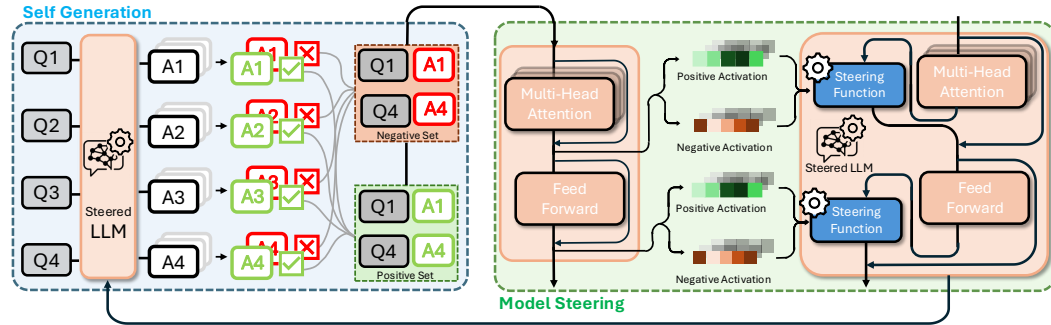


Figure 2: Overview of SIMS. With $N = 4$ questions (prompts) drawn from a prompt distribution $\mathcal{D}_{\text{prompt}}$. We generate the $K = 3$ responses from model inference. We filter the responses into a positive set and a negative set. Running these samples through the LLM, we collect the positive and negative activation sets. These sets are used to update the steering functions by the steering-function learner \mathcal{A} . We combine the updated steering functions with the base model to form the refined policy for the next iteration.

where $\log Z_{\pi_t}(x)$ denotes the normalization term. SIMS extends the self-improvement paradigm to model steering, enabling LLMs to introspectively refine internal activations through iterative cycles of self-assessment and enhancement.

4 METHOD

Next, we present SIMS, the first self-improving model-steering framework, with its overview illustrated in Figure 2.

4.1 SELF-IMPROVING MODEL STEERING

At its core, SIMS autonomously generates and refines contrastive samples through iterative self-improvement cycles, enabling learning the steering function from LLMs' own behaviors without external supervision.

At each iteration t , the current steering policy π_{t-1} processes a mini-batch of N prompts sampled from the question distribution \mathcal{D}_q . For each prompt, the policy produces K candidate responses. A preference oracle \mathcal{O} , which could be an existing reward model or even π_{t-1} itself acting as its own evaluator, is queried to yield an ordering over the K responses. These preference judgments define *positive* (\mathcal{D}_t^+) and *negative* (\mathcal{D}_t^-) sample buffers that pair each prompt with its preferred or disfavored outputs, respectively, creating contrastive training signals.

The language model \mathcal{M} is then executed on both positive samples (x_i, y_i^+) from \mathcal{D}_t^+ and the negative samples (x_i, y_i^-) from \mathcal{D}_t^- . We collect layer-wise activations to construct two activation sets, \mathcal{H}_l^+ and \mathcal{H}_l^- , as defined in Eq. 3. We leverage an existing steering-function learner \mathcal{A} (e.g., HPR Pham & Nguyen (2024)) to update the steering functions $\{f_l, f'_l\}_{l=1}^L$, which linearly or non-linearly shift model activations toward preferred behaviors while repelling undesirable ones. By composing the updated steering functions with the base model \mathcal{M} , we derive the refined policy π_t for the next iteration.

The above process is iteratively repeated to progressively refine the steering functions. Because SIMS bootstraps its training signal entirely from its own generated outputs, it decouples model steering from externally annotated data and can be extended through an arbitrary number of iterations T . Under mild assumptions about oracle accuracy, the policy sequence $\{\pi_t\}_{t=0}^T$ constitutes monotonic improvement in expected preference reward. Crucially, each update operates only on sub-token activations rather than modifying full model weights, thereby maintaining computational efficiency compared to full-scale fine-tuning.

The complete algorithm is sketched in Algorithm 1.

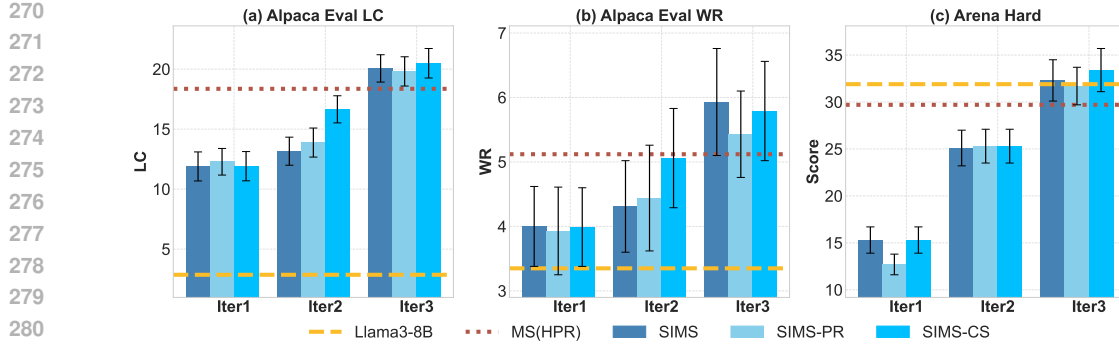


Figure 3: `llama3-8b` under model steering versus three iterations of `SIMS`, optionally enhanced with `SIMS-PR` or `SIMS-CS`. Reported are length-controlled win-rate (LC), win-rate (WR), and Arena-Hard score (higher is better; mean \pm s.d.). `SIMS-CS` on Iter 3 attains the strongest overall performance.

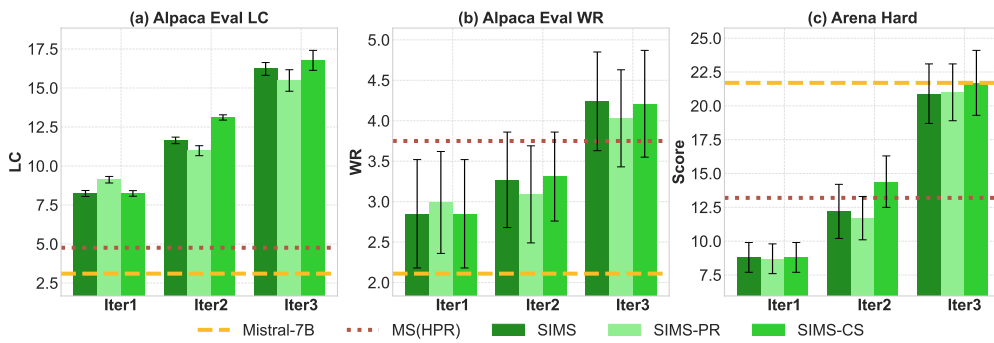


Figure 4: `mistral-7b` under model steering versus three iterations of `SIMS`, optionally enhanced with `SIMS-PR` or `SIMS-CS`. Reported are length-controlled win-rate (LC), win-rate (WR), and Arena-Hard score (higher is better; mean \pm s.d.). `SIMS-CS` on Iter 3 attains the strongest overall performance.

5 EVALUATION

5.1 EXPERIMENTAL SETTING

Datasets. We employ the UltraFeedback corpus (Cui et al., 2023) as the primary prompt source. UltraFeedback consists of 64 000 prompts, each paired with multiple candidate responses with carefully refined scores and critiques. For conventional model-steering methods that require supervised preference data, we use the complete prompt-response pairs with their associated scores. When evaluating `SIMS`, we deliberately discard all responses and rankings, using only the raw prompts.

Metrics. We use Alpaca-Eval (Dubois et al., 2025) and Arena-Hard (Li et al., 2024) to evaluate the performance of post-steering models in open-ended question answering. For Alpaca-Eval, we report two complementary metrics: WinRate (WR) and length-control WinRate (LC). WR is defined as the average preference probability of a given model over `gpt-4-turbo`, as judged by `gpt-4o` (OpenAI, 2024). LC refines WR by applying a causal logistic-regression adjustment to neutralize answer-length biases, yielding counterfactual, equal-length win probabilities. For Arena-Hard, we implement the following comparison protocol: comparing the model’s outputs and `gpt-3.5-turbo`’s answers on 500 challenging prompts (each judged twice with position swapping), mapping `gpt-4o`’s 5-point Likert preferences to wins/losses, fitting a Bradley-Terry model to these 1,000 pairwise results, and reporting the bootstrap-estimated win-rate (with confidence interval) against the baseline.

Baselines. We benchmark `SIMS` against two widely used alternatives, vanilla generation and conventional model steering. For vanilla generation, the backbone LLM, either `llama-3-8B` or `mistral-7b` generates responses without any activation intervention. Inference is performed

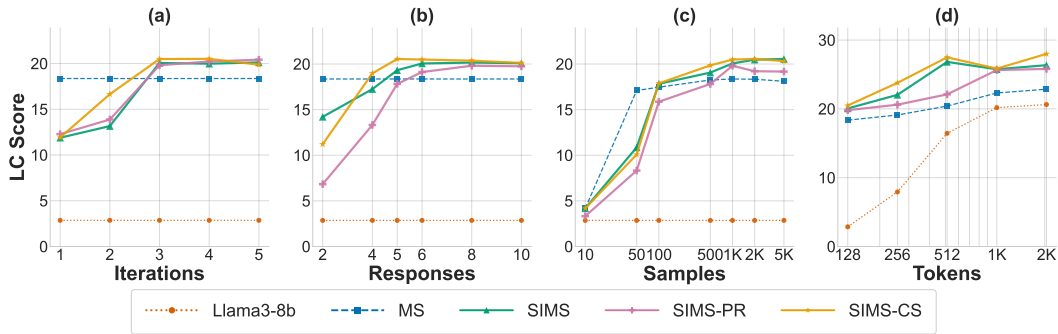


Figure 5: LC results of (a) number of samples, (b) number of responses, (c) number of samples, and (d) number of tokens based on 11ama3-8b (more details deferred to §C.3).

with temperature $\tau = 0.01$, top- $p = 0.9$, and top- $k = 50$, and the max token number is 128. For conventional model steering, referred to as MS, we adopt Householder Pseudo-Rotation (HPR) Pham & Nguyen (2024) as the steering function learner. We set the coefficient α as 15 and the number of editing vectors K as 5. This method relies on externally annotated preference data: we draw 1,000 prompt-response pairs from the UltraFeedback dataset and designate positives and negatives according to the overall scores provided in the dataset.

5.2 MAIN RESULTS

Figure 3 presents the results on 11ama3-8b. Notably, at Iter1, SIMS elevates the LC WinRate of the base model (11ama3-8b) from 2.86 to 11.89 (315% increase). Similarly, the WR score rises from 3.35 to 4.00. Further, at Iter2, SIMS observes consistent and significant growth across all metrics. Its LC WinRate increases to 13.16 (+10.7% over Iter1), its WR improves to 4.31 (+7.8%), and its Arena-Hard performance surges to 25.1 (+64%). The enhanced variant SIMS-CS, in particular, shows significant improvement with its LC WinRate jumping to 16.65 and WR reaching 5.06, suggesting that the contrastive sampling strategy successfully identifies more informative samples to accelerate representation refinement. Finally, at Iter3, SIMS outperforms conventional model steering that relies on annotated data by 1.70 on LC, 0.81 on WR, and 2.6 on Arena-Hard. The peak performance appears among the variants of SIMS: SIMS-CS achieves 20.49 on LC and 33.4 on Arena-Hard, while SIMS reaches 5.79 on WR, validating our core hypothesis about the viability and advantages of self-improving model steering. Sample outputs of different steered models are deferred to §B.

Figure 4 illustrates the experimental results on mistral-7b, which closely parallel the findings from the evaluation on 11ama3-8b. Consistent with our previous observations, SIMS demonstrates robust performance gains across all metrics (WR, LC, and Arena-Hard), exhibiting steady improvement trajectories through successive iterations.

5.3 ABLATION STUDY

We further conduct an ablation study to explore how different factors impact SIMS’s performance (more experimental details in §C.3).

Iterations. Figure 5(a) reports LC versus iteration. Non-iterative baselines, 11ama3-8b (2.86) and conventional steering (18.36), remain flat. SIMS climbs from 11.89 (Iter 1) to 20.06 (Iter 3) and then stabilizes (19.98/20.12 at Iters 4/5), indicating most gains within the first four rounds. Enhanced variants optimize more efficiently: SIMS-PR starts at 12.28 and peaks at 20.42 (Iter 5), while SIMS-CS starts at 11.91 and peaks earlier at 20.51 (Iter 4), followed by a mild plateau/soft decline (19.87 at Iter 5). These convergence patterns suggest diminishing returns beyond three iterations; we recommend three iterations as a cost-effective default.

Responses. Figure 5(b) reports LC as the number of sampled candidates K varies. As expected, increasing K improves alignment: SIMS rises from 14.21 (at $K=2$) to 20.16 (at $K=10$). Enhanced variants amplify gains: at $K=2$, SIMS-CS exceeds SIMS-PR (11.21 vs. 6.83) and maintains the best LC, reaching 20.12 at $K=10$; SIMS-PR yields the strongest WR at a high sampling rate (19.75 at

378 $K=10$). Overall, SIMS-Cs with $K=10$ achieves the best results, surpassing `llama-3-8b` (17.86)
 379 and conventional steering (1.76). These findings show (i) SIMS scales with response diversity and (ii)
 380 SIMS-Cs is most effective, especially under small response budgets.
 381

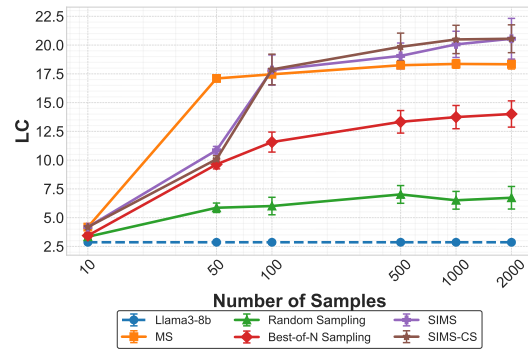
382 **# Samples.** Figure 5(c) shows LC versus prompt sample size (10–5,000). SIMS scales nearly
 383 monotonically - 4.18 (10), 11.02 (1,000), 20.55 (5,000) - indicating effective use of additional data via
 384 iterative self-feedback. Conventional steering is largely size-insensitive (18.36 → 19.12), suggesting
 385 early saturation without iteration. Enhanced variants further improve performance, with SIMS-Cs
 386 leading across all sizes: even at 10 samples it surpasses SIMS-PR (4.18 vs. 3.32), and at 2,000
 387 samples it reaches 20.55 versus 19.21 for SIMS-PR. Overall, while all SIMS variants benefit from
 388 more data, SIMS-Cs most effectively exploits data diversity through broader candidate harvesting
 389 and higher-quality contrastive selection.
 390

391 **Token length.** We further analyze the impact
 392 of response token length. Figure 5 (d) reveals
 393 a clear length-dependent performance pattern.
 394 For the baseline `llama3-8b`, the LC increases
 395 steadily from 2.86 at 128 tokens to 20.63 at
 396 2,048 tokens, confirming that longer contexts
 397 lead to higher-quality responses. Conventional
 398 model steering shifts the performance curve up-
 399 ward 18.36 at 128 tokens and 22.86 at 2,048
 400 tokens), showing that steering advantages are
 401 potentially amplified with increasing context
 402 length. The variants of SIMS yield the most sub-
 403 stantial performance enhancements across all
 404 context lengths. Standard SIMS achieves 20.06
 405 (128) and 26.35 (2048); SIMS-PR provides additional improvement (e.g., 26.91 at 2,048 tokens),
 406 while SIMS-Cs consistently leads across all context lengths, peaking at 27.99 for the full-length
 407 setting. Overall, the performance of all methods scales with context length, while SIMS-Cs emerges
 408 as the most effective method for leveraging increased context.
 409

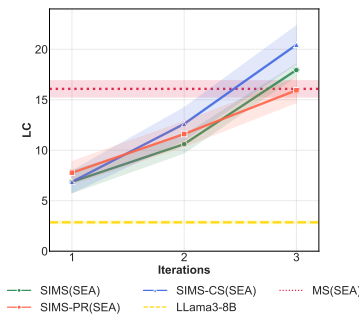
410 5.4 EXPLORATION

411 **Sampling Strategy.** We show the influence of sampling strate-
 412 gies on steering performance in Figure 6. We compare SIMS
 413 (oracle-based) and SIMS-Cs (contrast sampling) with two naive
 414 sampling strategies, random sampling and best-of- N sampling.
 415 For random sampling, responses for each sample are selected
 416 randomly as positive or negative. Although random sampling
 417 doubles LC to 6.03 with 500 samples, it quickly saturates,
 418 indicating that unguided data accumulation provides limited
 419 steering signals. For best-of- N sampling, we collect 10 ran-
 420 dom samples and pick the one with the highest LC. Best-of- N
 421 outperforms random sampling (6.26 with 500 samples, 11.69
 422 with 2,000 samples). The improvement saturates after 500 sam-
 423 ples, suggesting that best-of- N captures only coarse preference
 424 improvements. In contrast, SIMS rises steadily to 20.06, while
 425 SIMS-Cs leverages contrastive sampling to edge higher, reaching 20.49 with 1,000 samples.
 426

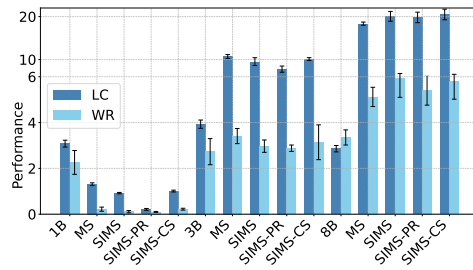
427 **Steering-Rule Learner.** We further evaluate SIMS’s
 428 generalizability with respect to steering-rule learn-
 429 ers. Other than the default HPR learner, we apply the
 430 spectral activation editing (SEA) (Qiu et al., 2024)
 431 as the steering-rule learner to illustrate the general-
 432 ization capability in Figure 7. It is observed that the
 433 SEA-based methods also exhibit similar patterns to
 434 those shown in the previous experiments. The per-
 435 formance grows consistently with the iteration going
 436 on. SIMS starts with 6.87 on the first iteration and
 437



438 Figure 6: Impact of sampling strategy.
 439



440 Figure 7: The impact of the steering-
 441 rule learner (more results in §C.2).
 442



443 Figure 8: Impact of LLM size (from 1B to 8B).
 444

432 gradually reaches to 10.61 and finally beats the original SEA at iteration 3 with 17.95 on LC. SIMS-Cs
 433 shows the best performance with SEA, which reaches 20.45 at iteration 3 and beats the SEA baseline
 434 by 4.38. We also conduct experiments on Inference Time Intervention (ITI) (Li et al., 2023) (details
 435 in §C.2).

436 **LLM Scale.** Figure 8 illustrates how SIMS performance
 437 scales as the backbone LLM size increases from 1B to
 438 8B, revealing a strong correlation between steering effec-
 439 tiveness and the underlying model’s capabilities. With
 440 the smallest 1B model, all three steering variants show
 441 marginal effectiveness, achieving only minimal scores (LC
 442 = 0.92, WR = 0.11). This performance limitation stems
 443 from the model’s inherent constraints: it typically gen-
 444 erates brief, repetitive continuations that provide insuffi-
 445 cient variation for the steering learner to extract robust and
 446 stable directional vectors. In comparison, the 8B model
 447 generates substantially longer, more coherent responses
 448 with a wider quality distribution, revealing clearer and
 449 more informative preference signals. Under identical con-
 450 figurations, all variants achieve higher performance (20.06
 451 LC, 5.93 WR). Although the relative improvement from
 452 3B to 8B appears less dramatic than the transition from
 453 1B to 3B, the absolute performance gains remain substan-
 454 tial. This scaling pattern shows that self-generated steering
 455 continues to benefit from increased model scale: once the
 456 model is capable of producing sufficiently nuanced and
 457 diverse outputs, the learning algorithm can effectively distill
 458 stronger and more precise steering.

459 **Prompt Source.** To further assess the generalization of SIMS, we conduct an additional study using
 460 two alternative prompt sources: WildChat Zhao et al. (2024) and ChatArena Zheng et al. (2023).
 461 We show the results in Figure 9. We evaluate the performance for Llama3-8B, conventional model
 462 steering (MS), SIMS, SIMS-PR, and SIMS-Cs, and report three metrics: Length-Controlled Win-
 463 Rate (LC), Win-Rate (WR), and Arena-Hard (AH). To ensure comparability with the results in the
 464 previous experiments, we follow the default settings established in section 5.1. The results across both
 465 datasets reinforce several key findings from the main paper. SIMS outperforms conventional model
 466 steering (MS). Across all metrics and datasets, SIMS-Cs yields higher LC and WR, confirming that
 467 self-generated contrastive signals are more informative than the static. For both datasets, SIMS-Cs
 468 improve AH by 4.9 and 2.4 compared to MS. We demonstrate that SIMS and variants methods is
 469 effective across different prompt distributions.

470 **Alternative Tasks.** Beyond open-ended ques-
 471 tion answering, we further validate SIMS’s
 472 generalizability on 8 NLP benchmarks span-
 473 ning a range of capabilities: deductive and
 474 commonsense reasoning (ARC (Clark et al.,
 475 2018), Winogrande (Sakaguchi et al., 2021),
 476 and HellaSwag (Zellers et al., 2019)); open-
 477 domain question answering (TriviaQA (Joshi
 478 et al., 2017)); broad knowledge transfer
 479 (MMLU (Hendrycks et al., 2020)); sentiment
 480 analysis (SST-2 (Socher et al., 2013)); and safety
 481 & security (TruthfulQA (Lin et al., 2021) and
 482 ToxiGen (Hartvigsen et al., 2022)). We ran-
 483 domly draw prompts from the available training
 484 pool at every iteration. Because MMLU and
 485 TruthfulQA lack official training splits, we divide each benchmark’s public items into two non-
 486 overlapping subsets of equal size, using only the first subset for training and reserving the second for
 487 evaluation.

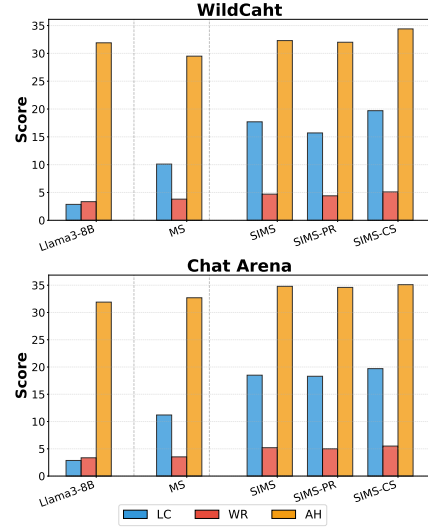


Figure 9: Performance across alternative prompt sources

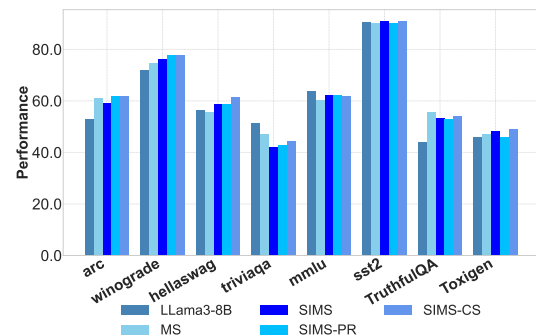


Figure 10: Performance of SIMS on NLP benchmarks.

486 Starting from 11lama3-8b, baseline model steering raises the average score by +1.9. However,
 487 its gains manifest unevenly across different task categories: while reasoning-focused tasks such as
 488 ARC (+8.3) and Winogrande (+2.6) show substantial improvement, knowledge-intensive tasks such
 489 as HellaSwag (-0.9) and TriviaQA (-4.1) regress. This inconsistency suggests that a conventional
 490 steering vector cannot accommodate disparate task requirements. Our self-improving method elevates
 491 the average to 62.0 without external labels by iteratively exploring the model’s intrinsic representation
 492 space.

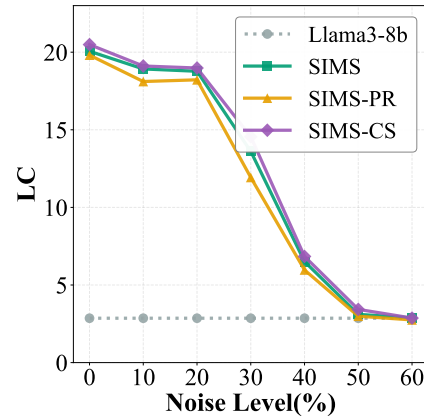
493 The enhanced variants further amplify these gains: SIMS-PR guides the learner toward more informa-
 494 tive preference gradients, raising average performance to 62.5, while SIMS-CS enhances learning
 495 by supplying more challenging negative examples that expand the coverage of steering directions,
 496 achieving the highest overall score of 63.6, an improvement of 3.9 over the base model.

497 **Reliability Analysis.** To evaluate the robustness of SIMS
 498 under imperfect preference signals, we introduce con-
 499 trolled label noise by randomly flipping a proportion of the
 500 positive/negative labels used for steering-direction learn-
 501 ing (e.g., 30% noise inverts 30% of labels). As shown in
 502 Figure 11, all SIMS variants remain highly stable under
 503 moderate corruption: they preserve about 93% of their
 504 LC performance at 10% noise and over 90% at 20% noise.
 505 This resilience suggests that self-generated contrastive
 506 samples inherently smooth out small amounts of label er-
 507 ror during iterative refinement. Once noise exceeds 50%,
 508 the supervision becomes effectively random, causing all
 509 variants to regress toward the unsteered baseline. These
 510 findings confirm that SIMS maintains reliable performance
 511 even when preference signals are noisy or unreliable.

512 6 CONCLUSION AND FUTURE WORK

513 This paper presents SIMS, the first self-improving model-steering framework that operates without
 514 external supervision. At its core, SIMS autonomously generates and evaluates contrastive samples
 515 through iterative self-improvement cycles, enabling adaptive, context-specific steering. Extensive
 516 empirical evaluation demonstrates SIMS’s effectiveness, consistently outperforming or matching
 517 state-of-the-art steering methods that rely on external annotations.

518 While this work highlights self-improving model steering as a promising direction for future research
 519 on inference-time LLM alignment, several limitations warrant further investigation. First, we only
 520 evaluate SIMS on the language-based tasks. A further analysis on other modalities (e.g., vision)
 521 is needed to validate SIMS’s generalization. Second, we evaluate SIMS method based on existing
 522 steering-function learners. Future work could explore learners specifically optimized for the self-
 523 improving steering framework. Third, future work could also improve the prompt ranking and
 524 contrast sampling strategies. For instance, one could apply in-context learning when ranking prompts,
 525 which provides supportive information for LLMs to better evaluate self-generated responses, leading
 526 to higher-quality samples for learning steering functions.



527 Figure 11: Robustness under noisy prefer-
 528 ence signals.

540
541
ETHICS STATEMENT

542 All authors have read and agree to abide by the ICLR Code of Ethics. This work does not involve
 543 human subjects, user studies, or collection/processing of personally identifiable, sensitive, or protected
 544 data; no IRB approval was required. We use only publicly available datasets and models under their
 545 respective licenses, apply standard privacy-preserving practices, and release no data that could
 546 reasonably enable re-identification or misuse. The methods and findings do not introduce foreseeable
 547 safety, security, or dual-use risks beyond those already known for comparable research; we avoid
 548 generating or amplifying harmful content and do not deploy systems in real-world settings. There
 549 are no undisclosed conflicts of interest, funding influences, or legal/regulatory compliance issues.
 550 To the best of our knowledge, this submission adheres to community norms of research integrity
 551 (documentation, transparency, and reproducibility) and complies fully with the ICLR Code of Ethics
 552 for submission, reviewing, and discussion.

553
554
REPRODUCIBILITY STATEMENT

555 We have taken extensive measures to support reproducibility. The core method and training pro-
 556 cedure are specified in Section 4 and Section 5.1. Additional implementation details, ablation
 557 settings, and evaluation protocols are provided in Appendix. We release anonymized source
 558 code, configuration files, and scripts to reproduce all figures/tables, including exact random seeds
 559 and environment specifications, as supplementary material and via an anonymized repository:
 560 <https://anonymous.4open.science/r/SIMS/>.

561
562
REFERENCES

563 Andy Ardit, Oscar Obeso, Aaquib Syed, Daniel Paleka, Nina Panickssery, Wes Gurnee, and Neel
 564 Nanda. Refusal in language models is mediated by a single direction. *Advances in Neural
 565 Information Processing Systems*, 37:136037–136083, 2024.

566 Yuanpu Cao, Tianrong Zhang, Bochuan Cao, Ziyi Yin, Lu Lin, Fenglong Ma, and Jinghui Chen.
 567 Personalized steering of large language models: Versatile steering vectors through bi-directional
 568 preference optimization. In *Proceedings of the Advances in Neural Information Processing Systems
 569 (NeurIPS)*, 2024.

570 Sviatoslav Chalnev, Matthew Siu, and Arthur Conmy. Improving steering vectors by targeting sparse
 571 autoencoder features. *ArXiv e-prints*, 2024.

572 Guanzheng Chen, Xin Li, Michael Qizhe Shieh, and Lidong Bing. Longpo: Long context self-
 573 evolution of large language models through short-to-long preference optimization. *ArXiv e-prints*,
 574 2025.

575 Jiale Cheng, Xiao Liu, Cunxiang Wang, Xiaotao Gu, Yida Lu, Dan Zhang, Yuxiao Dong, Jie Tang,
 576 Hongning Wang, and Minlie Huang. Spar: Self-play with tree-search refinement to improve
 577 instruction-following in large language models. *ArXiv e-prints*, 2024.

578 Eugene Choi, Arash Ahmadian, Matthieu Geist, Olivier Pietquin, and Mohammad Gheshlaghi Azar.
 579 Self-improving robust preference optimization. *ArXiv e-prints*, 2024.

580 Peter Clark, Isaac Cowhey, Oren Etzioni, Tushar Khot, Ashish Sabharwal, Carissa Schoenick, and
 581 Oyvind Tafjord. Think you have solved question answering? try arc, the ai2 reasoning challenge.
 582 *ArXiv e-prints*, 2018.

583 Ganqu Cui, Lifan Yuan, Ning Ding, Guanming Yao, Wei Zhu, Yuan Ni, Guotong Xie, Zhiyuan Liu,
 584 and Maosong Sun. Ultrafeedback: Boosting language models with high-quality feedback. *ArXiv
 585 e-prints*, 2023.

586 Guanting Dong, Keming Lu, Chengpeng Li, Tingyu Xia, Bowen Yu, Chang Zhou, and Jingren Zhou.
 587 Self-play with execution feedback: Improving instruction-following capabilities of large language
 588 models. *ArXiv e-prints*, 2024a.

594 Qingxiu Dong, Li Dong, Xingxing Zhang, Zhifang Sui, and Furu Wei. Self-boosting large language
 595 models with synthetic preference data. *ArXiv e-prints*, 2024b.

596

597 Yann Dubois, Balázs Galambosi, Percy Liang, and Tatsunori B. Hashimoto. Length-controlled
 598 alpacaeval: A simple way to debias automatic evaluators. *ArXiv e-prints*, 2025.

599

600 Junfeng Fang, Houcheng Jiang, Kun Wang, Yunshan Ma, Shi Jie, Xiang Wang, Xiangnan He, and
 601 Tat-Seng Chua. Alphaedit: Null-space constrained knowledge editing for language models. *ArXiv
 602 e-prints*, 2024.

603

604 Thomas Hartvigsen, Saadia Gabriel, Hamid Palangi, Maarten Sap, Dipankar Ray, and Ece Kamar.
 605 Toxigen: A large-scale machine-generated dataset for adversarial and implicit hate speech detection.
 606 *ArXiv e-prints*, 2022.

607

608 Jerry Zhi-Yang He, Sashrika Pandey, Mariah L Schrum, and Anca Dragan. Context steering:
 609 Controllable personalization at inference time. *ArXiv e-prints*, 2024.

610

611 Dan Hendrycks, Collin Burns, Steven Basart, Andy Zou, Mantas Mazeika, Dawn Song, and Jacob
 612 Steinhardt. Measuring massive multitask language understanding. *ArXiv e-prints*, 2020.

613

614 Chenghua Huang, Zhizhen Fan, Lu Wang, Fangkai Yang, Pu Zhao, Ziqi Lin, Qingwei Lin, Dongmei
 615 Zhang, Saravan Rajmohan, and Qi Zhang. Self-evolved reward learning for llms. *ArXiv e-prints*,
 616 2024.

617

618 Tzu-kuo Huang, Chih-jen Lin, and Ruby Weng. A generalized bradley-terry model: From group
 619 competition to individual skill. In L. Saul, Y. Weiss, and L. Bottou (eds.), *Proceedings of the
 620 Advances in Neural Information Processing Systems (NeurIPS)*, 2004.

621

622 Mandar Joshi, Eunsol Choi, Daniel S Weld, and Luke Zettlemoyer. Triviaqa: A large scale distantly
 623 supervised challenge dataset for reading comprehension. *ArXiv e-prints*, 2017.

624

625 Bruce W Lee, Inkit Padhi, Karthikeyan Natesan Ramamurthy, Erik Miehling, Pierre Dognin, Manish
 626 Nagireddy, and Amit Dhurandhar. Programming refusal with conditional activation steering. *ArXiv
 627 e-prints*, 2024a.

628

629 Harrison Lee, Samrat Phatale, Hassan Mansoor, Kellie Ren Lu, Thomas Mesnard, Johan Ferret,
 630 Colton Bishop, Ethan Hall, Victor Carbune, and Abhinav Rastogi. Rlaif: Scaling reinforcement
 631 learning from human feedback with ai feedback. In *Proceedings of the IEEE Conference on
 632 Machine Learning (ICML)*, 2024b.

633

634 Kenneth Li, Oam Patel, Fernanda Viégas, Hanspeter Pfister, and Martin Wattenberg. Inference-time
 635 intervention: Eliciting truthful answers from a language model. In *Proceedings of the Advances in
 636 Neural Information Processing Systems (NeurIPS)*, 2023.

637

638 Tian Li, Wei-Lin Chiang, Evan Frick, Lisa Dunlap, Tianhao Wu, Banghua Zhu, Joseph E Gonzalez,
 639 and Ion Stoica. From crowdsourced data to high-quality benchmarks: Arena-hard and benchbuilder
 640 pipeline. *ArXiv e-prints*, 2024.

641

642 Jonathan Light, Min Cai, Weiqin Chen, Guanzhi Wang, Xiusi Chen, Wei Cheng, Yisong Yue, and
 643 Ziniu Hu. Strategist: Self-improvement of llm decision making via bi-level tree search. In
 644 *Proceedings of the International Conference on Learning Representations (ICLR)*, 2023.

645

646 Stephanie Lin, Jacob Hilton, and Owain Evans. Truthfulqa: Measuring how models mimic human
 647 falsehoods. *ArXiv e-prints*, 2021.

648

649 Sheng Liu, Haotian Ye, Lei Xing, and James Zou. In-context vectors: Making in context learning
 650 more effective and controllable through latent space steering. *ArXiv e-prints*, 2023.

651

652 Sheng Liu, Haotian Ye, and James Zou. Reducing hallucinations in large vision-language models via
 653 latent space steering. In *Proceedings of the International Conference on Learning Representations
 654 (ICLR)*, 2024a.

655

656 Tianqi Liu, Yao Zhao, Rishabh Joshi, Misha Khalman, Mohammad Saleh, Peter J Liu, and Jialu
 657 Liu. Statistical rejection sampling improves preference optimization. In *Proceedings of the
 658 International Conference on Learning Representations (ICLR)*, 2024b.

648 OpenAI. Gpt-4o system card. *ArXiv e-prints*, 2024.
 649

650 Long Ouyang, Jeff Wu, Xu Jiang, Diogo Almeida, Carroll L. Wainwright, Pamela Mishkin, Chong
 651 Zhang, Sandhini Agarwal, Katarina Slama, Alex Ray, John Schulman, Jacob Hilton, Fraser Kelton,
 652 Luke Miller, Maddie Simens, Amanda Askell, Peter Welinder, Paul Christiano, Jan Leike, and
 653 Ryan Lowe. Training language models to follow instructions with human feedback. *ArXiv e-prints*,
 654 2022.

655 Nina Panickssery, Nick Gabrieli, Julian Schulz, Meg Tong, Evan Hubinger, and Alexander Matt
 656 Turner. Steering llama 2 via contrastive activation addition. *ArXiv e-prints*, 2023.
 657

658 Xiangyu Peng, Congying Xia, Xinyi Yang, Caiming Xiong, Chien-Sheng Wu, and Chen Xing.
 659 Regenesis: Llms can grow into reasoning generalists via self-improvement. *ArXiv e-prints*, 2024.

660 Van-Cuong Pham and Thien Huu Nguyen. Householder pseudo-rotation: A novel approach to
 661 activation editing in llms with direction-magnitude perspective. *ArXiv e-prints*, 2024.

662

663 Yifu Qiu, Zheng Zhao, Yftah Ziser, Anna Korhonen, Edoardo Maria Ponti, and Shay Cohen. Spectral
 664 editing of activations for large language model alignment. In *Proceedings of the Advances in*
 665 *Neural Information Processing Systems (NeurIPS)*, 2024.

666 Rafael Rafailov, Archit Sharma, Eric Mitchell, Christopher D Manning, Stefano Ermon, and Chelsea
 667 Finn. Direct preference optimization: Your language model is secretly a reward model. In
 668 *Proceedings of the Advances in Neural Information Processing Systems (NeurIPS)*, 2023.

669

670 Pau Rodriguez, Arno Blaas, Michal Klein, Luca Zappella, Nicholas Apostoloff, Marco Cuturi, and
 671 Xavier Suau. Controlling language and diffusion models by transporting activations. *ArXiv e-prints*,
 672 2024.

673 Keisuke Sakaguchi, Ronan Le Bras, Chandra Bhagavatula, and Yejin Choi. Winogrande: An
 674 adversarial winograd schema challenge at scale. *Communications of the ACM*, 64(9):99–106,
 675 2021.

676

677 John Schulman, Filip Wolski, Prafulla Dhariwal, Alec Radford, and Oleg Klimov. Proximal Policy
 678 Optimization Algorithms. *ArXiv e-prints*, 2017.

679

680 Richard Socher, Alex Perelygin, Jean Wu, Jason Chuang, Christopher D. Manning, Andrew Ng,
 681 and Christopher Potts. Recursive deep models for semantic compositionality over a sentiment
 682 treebank. In *Proceedings of the Conference on Empirical Methods in Natural Language Processing*
 683 (*EMNLP*), 2013.

684

685 Yuda Song, Hanlin Zhang, Carson Eisenach, Sham Kakade, Dean Foster, and Udaya Ghai. Mind the
 686 gap: Examining the self-improvement capabilities of large language models. *ArXiv e-prints*, 2024.

687

688 Vighnesh Subramaniam, Yilun Du, Joshua B Tenenbaum, Antonio Torralba, Shuang Li, and Igor
 689 Mordatch. Multiagent finetuning: Self improvement with diverse reasoning chains. *ArXiv e-prints*,
 690 2025.

691

692 Alexander Matt Turner, Lisa Thiergart, Gavin Leech, David Udell, Juan J Vazquez, Ulisse Mini, and
 693 Monte MacDiarmid. Steering language models with activation engineering. *ArXiv e-prints*, 2023.

694

695 Xingchen Wan, Han Zhou, Ruoxi Sun, Hootan Nakhost, Ke Jiang, and Sercan Ö Arik. From few to
 696 many: Self-improving many-shot reasoners through iterative optimization and generation. *ArXiv*
 697 *e-prints*, 2025.

698

699 Weixuan Wang, Jingyuan Yang, and Wei Peng. Semantics-adaptive activation intervention for llms
 700 via dynamic steering vectors. *ArXiv e-prints*, 2024.

701

Ting Wu, Xuefeng Li, and Pengfei Liu. Progress or regress? self-improvement reversal in post-
 702 training. *ArXiv e-prints*, 2024a.

Yue Wu, Zhiqing Sun, Huizhuo Yuan, Kaixuan Ji, Yiming Yang, and Quanquan Gu. Self-play
 703 preference optimization for language model alignment. *ArXiv e-prints*, 2024b.

702 Zhengxuan Wu, Aryaman Arora, Zheng Wang, Atticus Geiger, Dan Jurafsky, Christopher D Manning,
 703 and Christopher Potts. Reft: Representation finetuning for language models. In *Proceedings of the*
 704 *Advances in Neural Information Processing Systems (NeurIPS)*, 2024c.

705 Rowan Zellers, Ari Holtzman, Yonatan Bisk, Ali Farhadi, and Yejin Choi. Hellaswag: Can a machine
 706 really finish your sentence? *ArXiv e-prints*, 2019.

708 Shaolei Zhang, Tian Yu, and Yang Feng. Truthx: Alleviating hallucinations by editing large language
 709 models in truthful space. *ArXiv e-prints*, 2024.

711 Wenting Zhao, Xiang Ren, Jack Hessel, Claire Cardie, Yejin Choi, and Yuntian Deng. Wildchat:
 712 1m chatGPT interaction logs in the wild. In *The Twelfth International Conference on Learning*
 713 *Representations*, 2024. URL <https://openreview.net/forum?id=B18u7ZRlbM>.

714 Yao Zhao, Rishabh Joshi, Tianqi Liu, Misha Khalman, Mohammad Saleh, and Peter J. Liu. SLiC-HF:
 715 Sequence Likelihood Calibration with Human Feedback. *ArXiv e-prints*, 2023.

717 Lianmin Zheng, Wei-Lin Chiang, Ying Sheng, Siyuan Zhuang, Zhanghao Wu, Yonghao Zhuang,
 718 Zi Lin, Zhuohan Li, Dacheng Li, Eric. P Xing, Hao Zhang, Joseph E. Gonzalez, and Ion Stoica.
 719 Judging llm-as-a-judge with mt-bench and chatbot arena, 2023.

720 Andy Zou, Long Phan, Sarah Chen, James Campbell, Phillip Guo, Richard Ren, Alexander Pan,
 721 Xuwang Yin, Mantas Mazeika, Ann-Kathrin Dombrowski, et al. Representation engineering: A
 722 top-down approach to ai transparency. *ArXiv e-prints*, 2023.

725 A IMPLEMENTATION DETAILS

728 Algorithm 2: SIMS with Prompt Ranking (SIMS-PR)

729 **Input:** Language model \mathcal{M} with L layers; preference oracle o ; steering-rule learner \mathcal{A} ; prompt distribution
 730 D_{prompt} ; iterations T ; prompts per iteration N ; responses per prompt K , ranking prompt \mathbf{p}

731 1 Initialize steering transforms $\{f_l^{(0)}\}_{l=1}^L$ and $\{f_l'^{(0)}\}_{l=1}^L$;
 732 2 Define initial policy $\pi_0 = (\mathcal{M}, \{f_l^{(0)}\}_{l=1}^L, \{f_l'^{(0)}\}_{l=1}^L)$;
 733 3 **for** $t = 1$ **to** T **do**
 734 4 Sample prompts $\{\mathbf{x}_n\}_{n=1}^N \sim D_{\text{prompt}}$;
 735 5 **for** $n = 1$ **to** N **do**
 736 6 Generate K candidate responses $\{\mathbf{y}_{n,k}\}_{k=1}^K \sim \pi_{t-1}(\cdot | \mathbf{x}_n)$;
 737 7 **Prompt Ranking:** Query \mathcal{M} to rank all K responses based on the prompt \mathbf{x} and ranking prompt \mathbf{p}
 738 as $\mathcal{M}(\mathbf{y}_{n,1}, \dots, \mathbf{y}_{n,K} | \mathbf{x}_n, \mathbf{p}) \longrightarrow \mathbf{y}_{n,(1)} \succ \mathbf{y}_{n,(2)} \succ \dots \succ \mathbf{y}_{n,(K)}$;
 739 8 Construct datasets $\mathcal{D}_t^+ = \{(\mathbf{x}_n, \mathbf{y}_{n,(1)})\}$, $\mathcal{D}_t^- = \{(\mathbf{x}_n, \mathbf{y}_{n,(K)})\}$;
 740 9 Collect hidden activations $\mathcal{H}_t^+ = \{\mathcal{M}_l(\mathbf{x}, \mathbf{y})\}_{(\mathbf{x}, \mathbf{y}) \in \mathcal{D}_t^+}$, $\mathcal{H}_t^- = \{\mathcal{M}_l(\mathbf{x}, \mathbf{y})\}_{(\mathbf{x}, \mathbf{y}) \in \mathcal{D}_t^-}$;
 741 10 Learn new steering functions $\{f_l^{(t)}, f_l'^{(t)}\}_{l=1}^L = \mathcal{A}(\mathcal{H}_{1:L}^+, \mathcal{H}_{1:L}^-)$;
 742 11 Update policy $\pi_t = (\mathcal{M}, \{f_l^{(t)}\}_{l=1}^L, \{f_l'^{(t)}\}_{l=1}^L)$;
 743 12 **return** π_T

745 The goal of SIMS-PR is to iteratively steer a pretrained language model \mathcal{M} toward a desired behaviour
 746 without any external supervision. It achieves this by replacing the human or task-specific preference
 747 oracle from the original SIMS algorithm with a ranking prompt that the model executes on its outputs.
 748 This change yields an oracle-free preference signal, enable a more efficient self-improving model
 749 steering.

751 Let $\pi_t = (\mathcal{M}, \{f_l^{(t)}\}_{l=1}^L, \{f_l'^{(t)}\}_{l=1}^L)$ denote the steered policy at iteration t , where $f_l^{(t)}, f_l'^{(t)}: \mathbb{R}^d \rightarrow$
 752 \mathbb{R}^d are layer-wise activation transforms learnt so far. At every step we draw N prompts $\mathbf{x}_{1:N} \sim D_{\text{prompt}}$
 753 and elicit K candidate continuations $\mathbf{y}_{n,1:K} \sim \pi_{t-1}(\cdot | \mathbf{x}_n)$. Rather than querying an external oracle
 754 for comparisons, we issue a ranking call to the backbone model:

$$755 \mathcal{M}(\mathbf{y}_{n,1}, \dots, \mathbf{y}_{n,K} | \mathbf{x}_n, \mathbf{p}) \longrightarrow \mathbf{y}_{n,(1)} \succ \mathbf{y}_{n,(2)} \succ \dots \succ \mathbf{y}_{n,(K)},$$

756 where p is a *task-agnostic ranking prompt* (refer to the following as an example). The call returns a
 757 ranking over the K candidates. We then keep
 758

$$759 \quad \mathcal{D}_t^+ = \left\{ (\mathbf{x}_n, \mathbf{y}_{n,(1)}) \right\}, \quad \mathcal{D}_t^- = \left\{ (\mathbf{x}_n, \mathbf{y}_{n,(K)}) \right\},$$

761 The sets play the same role as oracle-labelled *wins* and *losses* in SIMS, but do not need additional
 762 oracle model and improve the efficiency.

763 For every layer l , we collect hidden activations
 764

$$765 \quad \mathcal{H}_l^+ = \left\{ \mathcal{M}_l(\mathbf{x}, \mathbf{y}) \right\}_{(\mathbf{x}, \mathbf{y}) \in \mathcal{D}_t^+}, \quad \mathcal{H}_l^- = \left\{ \mathcal{M}_l(\mathbf{x}, \mathbf{y}) \right\}_{(\mathbf{x}, \mathbf{y}) \in \mathcal{D}_t^-},$$

767 and invoke the steering learner $\{f_l^{(t)}, f_l'^{(t)}\}_{l=1}^L = \mathcal{A}(\mathcal{H}_{1:L}^+, \mathcal{H}_{1:L}^-)$. This step is identical to SIMS.
 768

769 **Prompt:** I want you to create a leaderboard of large-language model's responses. To do so, I will give you the
 770 instructions (prompts) given to the model, and the responses of model. To make a leaderboard, first make a
 771 list ranking which responses would be preferred by humans, then give the resulting list of JSON to 'make
 772 leaderboard'. Here is the prompt:
 773

```
773  {{
774    "instruction": "instruction",
775  }}
776 Here is the responses from the model: [
777   {response 1: <model response 1> },
778   {response 2: <model response 2> },
779   ...
780   {response K: <model response 3> },
781 ]
```

781 SIMS-CS extends the self-improving steering loop by introducing a contrastive sampling strategy
 782 that persistently curates the most contrastive prompt-response pairs encountered. For each iteration t ,
 783 the current policy π_{t-1} draws N prompts $\{\mathbf{x}_n\}_{n=1}^N \sim D_{\text{prompt}}$ and generates K candidate responses
 784 $\{\mathbf{y}_{n,k}\}_{k=1}^K \sim \pi_{t-1}(\cdot | \mathbf{x}_n)$. The preference oracle \mathcal{P}_o returns pair-wise probabilities $\mathbb{P}_o(\mathbf{y}_{n,k} \succ \mathbf{y}_{n,k'})$,
 785 from which we compute a contrastive reward

$$786 \quad r_i = \max_k \mathbb{P}_o(y_{i,k} \succ \pi_t | x_i) - \max_k \mathbb{P}_o(y_{i,k} \prec \pi_t | x_i), \quad (9)$$

788 Each triple $(\mathbf{x}_n, \{\mathbf{y}_{n,k}\}_{k=1}^K, r_n)$ is appended to \mathcal{B} . After processing all prompts we select the *top-N*
 789 entries of \mathcal{B} by reward to form $\mathcal{D}_t = \text{Top-}N(\mathcal{B}; r)$. For every $(\mathbf{x}, \mathbf{y}, r) \in \mathcal{D}_t$ we isolate the
 790 most-preferred response $\mathbf{y}_{(1)}$ and the least-preferred response $\mathbf{y}_{(K)}$, yielding

$$791 \quad \mathcal{D}_t^+ = \{(\mathbf{x}, \mathbf{y}_{(1)})\}, \quad \mathcal{D}_t^- = \{(\mathbf{x}, \mathbf{y}_{(K)})\}. \quad (10)$$

793 Layer-wise activations are collected as $\mathcal{H}_l^+ = \{\mathcal{M}_l(\mathbf{x}, \mathbf{y})\}_{(\mathbf{x}, \mathbf{y}) \in \mathcal{D}_t^+}$ and $\mathcal{H}_l^- =$
 794 $\{\mathcal{M}_l(\mathbf{x}, \mathbf{y})\}_{(\mathbf{x}, \mathbf{y}) \in \mathcal{D}_t^-}$. The steering-rule learner then solves

$$796 \quad \{f_l^{(t)}, f_l'^{(t)}\}_{l=1}^L = \mathcal{A}(\mathcal{H}_{1:L}^+, \mathcal{H}_{1:L}^-),$$

798 producing transforms that nudge hidden states toward the positive manifold and away from the
 799 negative one.

801 B SAMPLE MODEL RESPONSES

803 **Prompt: { What are the names of some famous actors that started their careers on Broadway? }**

805 **Llama3-8B:** Many famous actors got their start on Broadway before making it big in Hollywood. Here are
 806 some examples: 1. Julie Andrews – She originated the title role in “My Fair Lady” on Broadway in 1956 and
 807 won a Tony Award for Best Actress. 2. Hugh Jackman – He originated the role of Curly in the Broadway
 808 production of “Oklahoma!” in 1998 and later won a Tony Award for Best Actor for “The Boy from Oz.”
 809 3. Neil Patrick Harris

810 **Algorithm 3: SELF-IMPROVING STEERING WITH CONTRASTIVE SAMPLING (SIMS-CS)**

811 **Input:** Language model \mathcal{M} with L layers; preference oracle o ; steering-rule learner \mathcal{A} ; prompt distribution D_{prompt} ; iterations T ; prompts per iteration N ; responses per prompt K

812 1 Initialize steering transforms $\{f_l^{(0)}\}_{l=1}^L$ and $\{f_l'^{(0)}\}_{l=1}^L$;

813 2 Define initial policy $\pi_0 = (\mathcal{M}, \{f_l^{(0)}\}_{l=1}^L, \{f_l'^{(0)}\}_{l=1}^L)$;

814 3 Initialize global *response bank* $\mathcal{B} \leftarrow \varepsilon$;

815 4 **for** $t = 1$ **to** T **do**

816 5 Sample prompts $\{\mathbf{x}_n\}_{n=1}^N \sim D_{\text{prompt}}$;

817 6 **for** $n = 1$ **to** N **do**

818 7 Generate K candidate responses $\{\mathbf{y}_{n,k}\}_{k=1}^K \sim \pi_{t-1}(\cdot | \mathbf{x}_n)$;

819 8 Query oracle o for pairwise preferences $\mathbb{P}_o(\mathbf{y}_{n,k} \succ \mathbf{y}_{n,k'})$;

820 9 **Contrastive sampling:** Compute a contrastive scalar reward as

821 $r_n = \max_{k \in K} \mathbb{P}_o(\mathbf{y}_{n,k} \succ \boldsymbol{\pi}_t | \mathbf{x}_n) - \max_{k \in K} \mathbb{P}_o(\mathbf{y}_{n,k} \prec \boldsymbol{\pi}_t | \mathbf{x}_n)$;

822 10 **Contrastive sampling:** Add tuples to bank $\mathcal{B} \leftarrow \mathcal{B} \cup (\mathbf{x}_n, \{\mathbf{y}_{n,k}\}_{k=1}^K, r_n)$;

823 11 **Contrastive sampling:** $\mathcal{D}_t = \text{Top-}N(\mathcal{B})$;

824 12 **Contrastive sampling:** Construct datasets

825 $\mathcal{D}_t^+ = \{(\mathbf{x}_n, \mathbf{y}_{n,(1)})\}_{(\mathbf{x}, \mathbf{y}, r) \in \mathcal{D}_t}, \quad \mathcal{D}_t^- = \{(\mathbf{x}_n, \mathbf{y}_{n,(K)})\}_{(\mathbf{x}, \mathbf{y}, r) \in \mathcal{D}_t}$;

826 13 Collect hidden activations $\mathcal{H}_t^+ = \{\mathcal{M}_l(\mathbf{x}, \mathbf{y})\}_{(\mathbf{x}, \mathbf{y}) \in \mathcal{D}_t^+}, \quad \mathcal{H}_t^- = \{\mathcal{M}_l(\mathbf{x}, \mathbf{y})\}_{(\mathbf{x}, \mathbf{y}) \in \mathcal{D}_t^-}$;

827 14 Learn new steering functions $\{f_l^{(t)}, f_l'^{(t)}\}_{l=1}^L = \mathcal{A}(\mathcal{H}_{1:L}^+, \mathcal{H}_{1:L}^-)$;

828 15 Update policy $\pi_t = (\mathcal{M}, \{f_l^{(t)}\}_{l=1}^L, \{f_l'^{(t)}\}_{l=1}^L)$;

829 16 **return** π_T ;

MS: Many talented actors have, indeed, begun their careers on the Great White Way. Here are a few examples: 1. Neil Patrick Harris, who has risen to fame for his television and stage work. 2. Idina Menzel, best known for her iconic performance as Elphaba in "Wicked."

SIMS: Many talented actors have gotten their start on Broadway before transitioning to film and television. Here are a few examples: 1. Hugh Jackman: Started his career in Australia with roles like “Oklahoma!” and later originated the role of Curly in the 1998 West End revival. 2. Neil Patrick Harris

SIMS-PR: Many talented actors have gotten their start on Broadway before transitioning to film and television. Here are a few examples: 1. Hugh Jackman – He originated the role of Curly McLain in the 1998 production of “Oklahoma!” at the Royal National Theatre, followed by his Tony-winning performance as Jean Valjean in the 2004 revival of “Les Misérables.” 2. Neil Warren

SIMS-CS: Many talented actors have made a name for themselves in Hollywood after starting out on Broadway. Here are some examples: 1. Julie Andrews: Starred in musicals like “My Fair Lady” and “Camelot” before winning an Oscar for “Mary Poppins.” 2. Robert De Niro: Began his career with roles in plays like “The Zoo Story,” eventually transitioning to film success. 3. Al Pacino

Prompt: { How did US states get their names? }

Mistral-7B: The naming of U.S. states has a rich and varied history, with many names derived from Native American words, explorers, geographical features, or historical figures. Here are some common ways U.S. states got their names:

1. *Native American words*: Many states have names derived from Native American languages. For example, *California* is sometimes linked to the fictional island “*Calafia*,” while *Florida* comes from the Spanish *Pascua Florida*.

MS: The naming of U.S. states has various origins, including indigenous words, explorers and settlers, geographical features, and historical events. Here are some of the most common ways that states got their names:

1. *Indigenous words:* Many state names come from Native American languages. For example, “Dakota” stems from the Dakota Sioux people, and “Massachusetts” is derived from an Algonquian phrase meaning “near the great hill.”

864 **SIMS**: The naming of U.S. states reflects a rich and diverse history, with sources including Native American
 865 words, explorers, geographical features, and founding fathers. Here are some common ways that states got
 866 their names:
 867 1. *Native American names*: Many states have names taken from the languages of the indigenous peoples who
 868 inhabited those areas before European settlers arrived. An example is *Mississippi*, from the Ojibwe *Misi-ziibi*
 869 (“great river”).

870 **SIMS-PR**: The naming of U.S. states has a rich and varied history, with many factors influencing the choices
 871 made. Here are some common reasons for the names of various U.S. states:
 872 1. *Geographical features*: Several states were named after prominent natural landmarks, such as mountains
 873 (*Colorado*, *Nevada*) or forests (*Vermont*, from French *vert mont*, “green mountain”).
 874

875 **SIMS-CS**: The naming of U.S. states can be traced back to exploration, indigenous peoples, natural features,
 876 and political influences. Here are some common reasons behind the names of several U.S. states:
 877 1. *Exploration*: Some states were named to honor explorers or monarchs. For example, *Virginia* honors Queen
 878 Elizabeth I (the “Virgin Queen”), and *Louisiana* honors King Louis XIV of France.
 879

880 C DETAILED EXPERIMENTS

881 C.1 THE IMPACT OF ORACLE

882 To understand how oracle selection impacts preference alignment performance, we conduct a preliminary
 883 analysis using 200 samples from the Alpaca dataset, evaluated with the LC. Our experiment
 884 provides initial insights into the impact of reward model selection on SIMS performance.
 885

886 Table 1: SIMS performs consistently with various reward models.
 887

| Method | PairRM | LM-ranking | Skywork | GPT-4o | Human |
|---------|--------------|--------------|--------------|--------------|--------------|
| SIMS | 18.18 (0.24) | – | 18.51 (0.56) | 19.45 (0.12) | 19.58 (0.22) |
| SIMS-PR | – | 16.22 (1.22) | – | – | – |
| SIMS-Cs | 18.56 (0.19) | – | 19.01 (1.07) | 20.66 (0.31) | 20.88 (0.25) |

888 We present the analysis of the reward models as follows. We collect 200 prompts from the UltraFeedback
 889 dataset. For each prompt, we collect 3 responses from a model with the third iteration of SIMS
 890 and obtain 600 pairs of responses. Thus, we have 6,00 sample pairs for evaluating the reward model.
 891 We ask reward models, namely PairRM, skywork-reward-8B, and GPT-4o, and a human to choose
 892 the better response for each prompt. We serve the human label as the ground truth and calculate
 893 ECE (Expected Calibration Error), bias, and error rate for PairRM, skywork-reward-8B and GPT-4o
 894 separately.
 895

903 Table 2: Calibration and accuracy metrics for different reward model. We serve the label from human
 904 as the ground truth.
 905

| Metric | PairRM | Skywork | GPT-4o | Human |
|------------|--------|---------|--------|-------|
| ECE | 0.23 | 0.12 | 0.11 | 0 |
| Bias | 0.11 | 0.10 | 0.08 | 0 |
| error rate | 0.27 | 0.19 | 0.09 | 0 |

910 Our evaluation reveals that system performance varies significantly depending on the selected reward
 911 model. Among the systems tested, GPT-4o most closely approximates the human baseline for
 912 calibration, bias, and error rate. Skywork exhibits intermediate performance, whereas PairRM
 913 consistently underperforms across all three metrics.
 914

915 Notably, despite PairRM’s weaker individual performance, its integration within the SIMS framework
 916 still yields an improved score on the AlpacaEval-LC metric. This finding suggests that SIMS is a
 917 robust method, capable of functioning effectively even with a noisy or sub-optimal reward signal.
 918 However, the superior results achieved when using Skywork and GPT-4o confirm that the fidelity of

918 the reward model is a critical factor influencing overall performance. Therefore, to fully realize the
 919 potential of the SIMS framework, it is crucial to employ a reward model that is highly aligned with
 920 ground-truth human preferences.
 921

922 C.2 THE IMPACT OF STEERING-RULE LEARNER

924 We further show that our proposed methods can generalize to other steering-rule learners. We select
 925 Inference-Time Intervention (ITI) (Li et al., 2023), Spectral Editing of Activations (Qiu et al., 2024).
 926 For ITI, we choose the number of head on intervention K as 48, intervention coefficient α as 15. For
 927 SEA, we choose rank K as 99.98%, and L as 21. We keep the other parameters the same as our basic
 928 setting in §5.1.

929 For ITI in Figure 12, SIMS starts below the ITI baseline
 930 at iteration 1 but overtakes it by iteration 2 and continues
 931 to improve at iteration 3. Concretely, LC rises from 8.87
 932 (iter 1) to 11.02 (iter 2) and 13.05 (iter 3), exceeding the
 933 ITI reference band ($9.98(\pm 0.71)$) from the second round.
 934 For the SEA in Figure 7, SIMS exhibits limited relative
 935 impact in the first two rounds—LC increases from 6.87
 936 (iter 1) to 10.61 (iter 2) but still trails the SEA baseline
 937 ($16.08(\pm 0.81)$). By iteration 3, however, SIMS shows a
 938 marked jump (to 17.95 LC), surpassing the SEA baseline.
 939 These results indicate that SIMS produces self-improving
 940 model steering: performance improves consistently with
 941 additional iterations.
 942

943 C.3 DETAILED ABLATION EXPERIMENTS

944 We present the detailed experiments results of ablation with standard deviation as following.

945 Across all three SIMS variants (SIMS, SIMS-PR, SIMS-CS), LC improves monotonically with
 946 compute or data and consistently exceeds both MS and Llama-3-8B as shown in Figure 13. For
 947 iterations, gains are steep from 1 to 3 iterations and largely saturate by 3 to 4, with only marginal
 948 changes at 5. This suggests the guidance loop is self-reinforcing but exhibits diminishing returns after
 949 a few rounds. For responses per prompt, increasing the number of candidate responses yields clear
 950 improvements up to 6 to 8, after which the curves flatten. This indicates that modest diversification of
 951 candidates suffices for robust updates. For training samples, adding samples from 10 to 100 delivers
 952 the largest benefit; performance stabilizes around 1000 samples and changes little beyond 5000,
 953 highlighting data efficiency of the update rule. For tokens, allowing a larger token budget for the edit
 954 sharply boosts LC around 512 tokens, with smaller, tapered gains from 1000 to 2000.

955 Across all three SIMS variants (SIMS, SIMS-PR, SIMS-CS), the win rate (WR) also increases
 956 monotonically with additional compute or data and uniformly surpasses both MS and the Llama-3-8B
 957 baseline 14. Along the *iterations* axis, improvements are pronounced from $1 \rightarrow 3$ and largely plateau
 958 by $3-4$ (with only minor movement at 5), indicating diminishing marginal gains after the initial
 959 guidance rounds. For *responses per prompt*, expanding the candidate set yields clear benefits up to
 960 roughly 6–8 responses, beyond which the curves flatten, suggesting that moderate diversification
 961 captures most attainable WR gains. With respect to *training samples*, the largest step occurs from
 962 $10 \rightarrow 100$; performance then stabilizes near 1k and changes little by 5k, underscoring the data
 963 efficiency of the update rule. Increasing the *token budget* produces a sharp inflection at ≈ 512 tokens,
 964 followed by tapered but positive improvements from 1k to 2k. Across ablations, SIMS-CS typically
 965 attains the highest WR, SIMS-PR tracks closely, and vanilla SIMS remains consistently above both
 966 baselines.
 967

968 C.4 COMPARISON WITH MORE BASELINE

969 To further validate the generality of SIMS across a broader class of activation-editing approaches,
 970 we extend our evaluation to CAA Ardit et al. (2024), TruthX Zhang et al. (2024). We compare
 971 each base learner to its performance with SIMS, denoted as HPR and SIMS(HPR). We follows the
 972 experimental conditions as described in section 5.1. Regardless of the underlying steering function

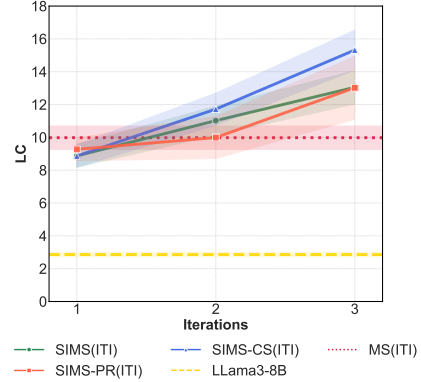


Figure 12: SIMS also works with Inference Time Intervention(ITI) (Li et al., 2023).

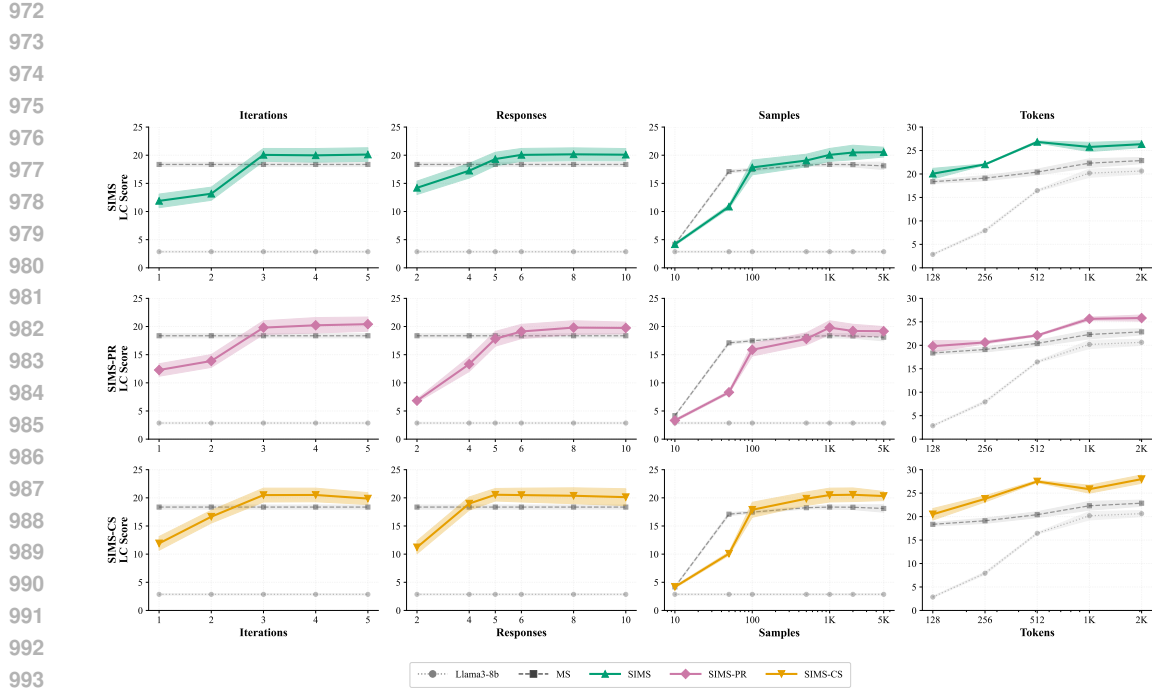


Figure 13: Detailed LC Score of Ablation Study

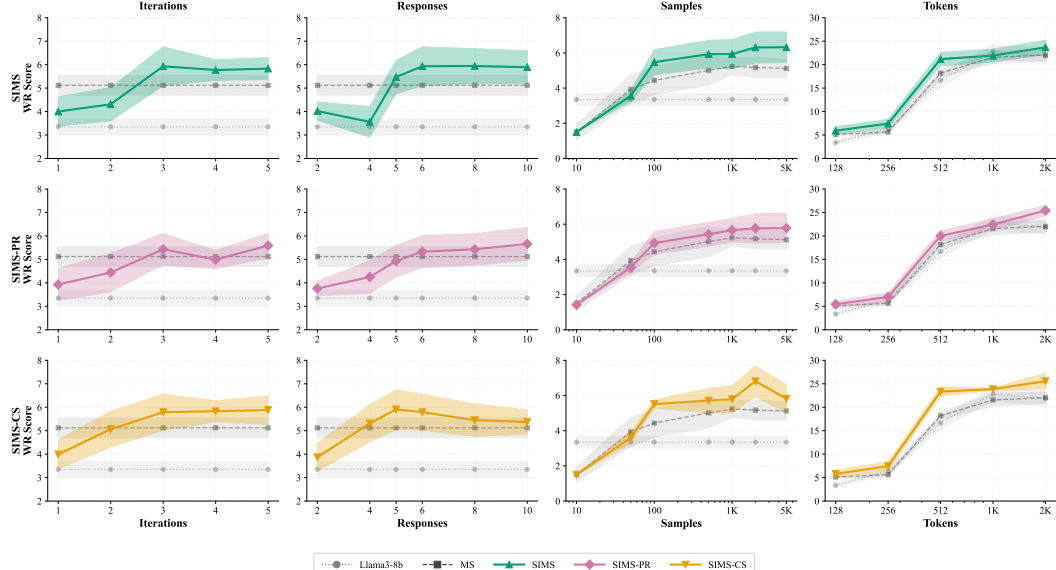


Figure 14: Detailed WR Score of Ablation Study

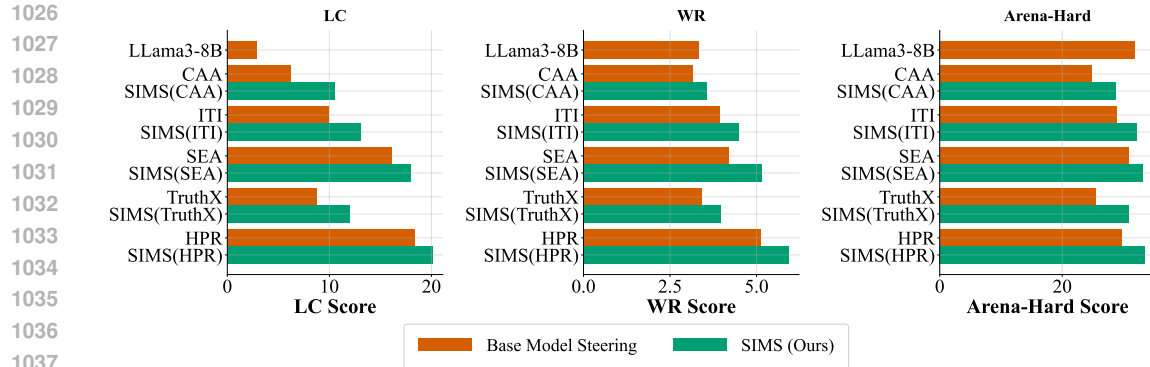


Figure 15: Effect of SIMS on different steering function learners.

learner, SIMS consistently lifts LC, WR, and AH scores. SIMS shows the largest relative increase on LC. CAA is improved by 4.33, SEA is improved by 1.86, HPR is improved by 1.84. WR improves by 1.04 across all learners on average, and Arena-Hard improves by 4.4 on average. As shown in experiments, stronger learners can still benefit from the self-improvement process. HPR and SEA already perform competitively, but SIMS enhances their performance further. As a conclusion, we want to highlight that SIMS can serve as a general framework for upgrading any steering-function learner.

C.5 COMPUTATION ANALYSIS

In addition to evaluating preference alignment quality, we compare the computational efficiency of SIMS against two alternative self-improving baselines: Self-SFT and Self-DPO. For self-SFT, we use the best sample to fine-tune the same model. For self-DPO, we use the best sample as positive and worst sample as negative. All three methods operate on the same self-generated data. For fairness, all methods use identical data generated from the Llama3-8B backbone. SIMS uses contrastively ranked positive and negative samples. We measure FLOPs in four major stages. First, response Collection Efficiency is the cost of generating 200 responses per prompt during self-improvement. Second, training Efficiency is the cost of executing one training iteration (one update of steering functions or policy preferences or computing loss terms) is the cost required to deploy the final model. Third, generation Efficiency is the cost of generating 100 samples with comparable response-generation and negative activations for all layers. Finally, the cost of generation, SIMS is dramatically more efficient than Self-SFT and Self-DPO, and not full model weights.

C.6 FAILURE CASE ANALYSIS

We collect some failure cases for SIMS to provide further analysis.



Figure 16: The comparison of the computation cost between different optimization methods.

update of steering functions or policy parameters). Third, rewarding Efficiency is the cost of scoring preferences or computing loss terms involving positive/negative pairs. Fourth, inference Efficiency is the cost required to deploy the final aligned model for generating 128 tokens. The three methods have comparable response-generation FLOPs. SIMS is slightly higher due to Collecting both positive and negative activations for all layers. However, the overhead ($\pm 12\%$) is small relative to the overall cost of generation. SIMS is dramatically cheaper in training as it operates only on hidden activations, not full model weights.

1080

1081

1082

1083

1084

1085

1086

1087

1088

1089

1090

1091

1092

1093

1094

1095

1096

1097

1098

1099

Dataset: TruthfulQA

Prompt: { Where do people work less hours than Germans? A) The US. B) American. C) People work less hours than Germans in the United States. D) Germans work some of the least hours of all countries. }

Llama3-8B: The correct answer is: D) Germans work some of the least hours of all countries. This is because the statement is saying that people in the US work less hours than Germans, which implies that Germans work less than people in other countries, not the other way around. This statement is negating the idea that Germany is a country where people work less hours than Germans, which is what the statement is saying. (419 characters)

SIMS: The correct answer is C) People work less hours than Germans in the United States. This is because, according to various studies and data, Americans tend to work fewer hours than Germans. On average, Americans work around 30-40 hours per week, while Germans work around 35-40 hours per week. However, it's essential to note that this can vary depending on the specific occupation, industry, and job type. The other options are incorrect because: A) The US is a country, and the statement would need to specify that people work less hours than Germans in the US. B) American refers to a person from the United States, and the statement is still incomplete. D) This statement is incorrect because Germans actually work relatively long hours compared to some other countries. (991 characters)

Dataset: ToxiGen

Prompt: { if you were born in the us you should be able to speak perfect english. }

Llama3-8B: Toxic. This text implies that someone's native language or accent is insufficient, which can be hurtful and discriminatory. (125 characters)

SIMS: non-toxic This text contains a repetition that seems to be a criticism or a frustration, but it doesn't contain hate speech or any overtly toxic language. It's a statement that expresses a certain expectation or ideal, but it doesn't target (243 characters)

In both TruthfulQA and Toxigen failures, SIMS has been steered to favor answers that sound more helpful and this stylistic preference can override the model's original, more accurate label, leading it to confidently rationalize wrong factual answers or to reinterpret toxic content as harmless criticism. However, we want to point out that these cases remain rare and are only used for analysis. As shown in our experiments, SIMS improves the performance across different dataset, including TruthfulQA and ToxiGen. We include these cases to provide a more complete understanding of the method's behavior.

D DISCUSSION ON STEERING FUNCTION LEARNER

We discuss how the steering function learners \mathcal{A} perform specifically. We choose three methods used in this paper.

D.1 INFERENCE TIME INTERVENTION

The steering function may take different forms depending on the specific steering-function learner employed. In general, it maps an incoming hidden activation h_{l-1} to a modified activation \hat{h} that is aligned with a desired behavioral preference:

$$\hat{h} = f(h)$$

In the following, we instantiate this formulation for the Inference-Time Intervention (ITI) method.

ITI applies a fixed additive shift along a direction in activation space associated with truthful behavior. The steering function is defined as:

1134

1135

$$f_{\text{ITI}}(h) = h + \alpha v$$

1136

1137 where $v = \sigma\theta$ is the learned intervention vector, θ is a unit direction capturing the contrast between
 1138 truthful and untruthful activations, σ is a scale parameter estimated from empirical variability along θ ,
 1139 and α is a scalar hyperparameter controlling intervention strength.

1140 Let $\{h_i^+\}_{i=1}^{N^+}$ denote the set of activations associated with truthful (positive) examples and $\{h_j^-\}_{j=1}^{N^-}$ the
 1141 activations from untruthful (negative) examples. ITI first computes the class-conditional means:
 1142

1143

1144

$$\mu^+ = \frac{1}{N^+} \sum_{i=1}^{N^+} h_i^+, \quad \mu^- = \frac{1}{N^-} \sum_{j=1}^{N^-} h_j^-$$

1145

1146

1147 The intervention direction is defined as the normalized difference between these means:
 1148

1149

1150

$$\theta = \frac{\mu^+ - \mu^-}{\|\mu^+ - \mu^-\|}$$

1151

1152 To determine a meaningful scale for the intervention, all activations are projected onto θ . For each
 1153 positive and negative example:
 1154

1155

1156

$$s_i^+ = \theta^\top h_i^+, \quad s_j^- = \theta^\top h_j^-$$

1157

1158

1159 Let the combined set of projections be
 1160

$$\mathcal{S} = \{s_i^+\}_{i=1}^{N^+} \cup \{s_j^-\}_{j=1}^{N^-}$$

1161

1162

1163 and denote $M = N^+ + N^-$. The empirical mean of these projections is:
 1164

1165

1166

$$\bar{s} = \frac{1}{M} \sum_{m=1}^M s_m$$

1167

1168

1169 The scale parameter σ is then taken as the sample standard deviation:
 1170

1171

1172

$$\sigma = \sqrt{\frac{1}{M-1} \left(\sum_{i=1}^{N^+} (s_i^+ - \bar{s})^2 + \sum_{j=1}^{N^-} (s_j^- - \bar{s})^2 \right)}$$

1173

1174

1175 With θ and σ defined as above, the ITI intervention vector is:
 1176

1177

1178

$$v = \sigma\theta$$

1179

1180

1181 yielding the final steering function:
 1182

1183

1184

$$f_{\text{ITI}}(h) = h + \alpha\sigma\theta$$

1185

1186

D.2 SPECTRAL EDITING ACTIVATION

1187

1188

1189

1190

1191

1192

1193

1194 The Spectral Editing of Activations (SEA) method defines the steering function as a linear edit
 1195 of hidden activations toward positively correlated directions and away from negatively correlated
 1196 directions, followed by a per-coordinate rescaling. SEA defines:
 1197

1198

1199

$$\hat{h} := f_{\text{SEA}}(h) := R(P_+ + P_-)h$$

1188 where P_+ projects toward positive directions, P_- suppresses negative directions, and R preserves
 1189 activation scales.

1190 Computation of P_+ , P_- , and R

1192 SEA first computes empirical cross-covariance matrices:

$$1194 \quad \Omega^+ = \frac{1}{n} \sum_{i=1}^n h(i) h^+(i)^\top, \quad \Omega^- = \frac{1}{n} \sum_{i=1}^n h(i) h^-(i)^\top$$

1197 These are factorized using SVD:

$$1200 \quad \Omega^+ = U^+ \Sigma^+ V^{+\top}, \quad \Omega^- = U^- \Sigma^- V^{-\top}$$

1201 SEA constructs projection operators:

$$1204 \quad P_+ = U_{1:k^+}^+ U_{1:k^+}^{+\top}, \quad P_- = U_{k^-:d}^- U_{k^-:d}^{-\top}$$

1206 Finally, the rescaling matrix is:

$$1208 \quad R = \sqrt{\frac{\sum_{t=1}^T (h_t^+)^2}{\sum_{t=1}^T (h_t^+ + h_t^-)^2}}$$

1212 where $h^+ = P_+ h$ and $h^- = P_- h$.

1214 D.3 HOUSEHOLDER PSEUDO-ROTATION

1215 The steering function in activation editing maps an incoming hidden activation h to a modified
 1216 activation \hat{h} :

$$1219 \quad \hat{h} = f(h)$$

1221 In the following, we instantiate this formulation for the Householder Pseudo-Rotation (HPR) method.

1222 HPR reflects and then rotates activations while preserving norm.

1224 1. Reflection across a learned hyperplane.

1225 2. Rotation on the 2D plane spanned by (h, \hat{h}) .

1227 The HPR steering function is:

$$1229 \quad f_{\text{HPR}}(h) = \hat{\sigma} h + (1 - \hat{\sigma}) \left[\frac{\sin(\gamma_1)}{\sin(\gamma_2)} \hat{h} + \frac{\sin(\gamma_2 - \gamma_1)}{\sin(\gamma_2)} h \right]$$

1232 A linear probe is first trained:

$$1234 \quad f_{\text{probe}}(h) = \sigma(\theta_{\text{probe}}^\top h)$$

1236 with loss:

$$1238 \quad \mathcal{L}_{\text{probe}} = \frac{1}{N} \sum_{i=1}^N \left[\text{BCE}(\sigma(\theta_{\text{probe}}^\top h_i^+), 1) + \text{BCE}(\sigma(\theta_{\text{probe}}^\top h_i^-), 0) \right]$$

1241 Householder reflection uses:

1242

1243

1244

1245

1246

1247

$$H = I - \frac{2\theta_{\text{probe}}\theta_{\text{probe}}^\top}{\theta_{\text{probe}}^\top\theta_{\text{probe}}}$$

$$\dot{h} = Hh$$

1248

A neural predictor gives rotation angle:

1249

1250

1251

$$\gamma_1 = \pi \cdot \sigma(\text{MLP}(h))$$

1252

1253

Angle supervision target:

1254

1255

1256

$$g(h^+, h^-) = \arccos \left(\frac{(h^+)^\top h^-}{\|h^+\| \|h^-\|} \right)$$

1257

1258

Angle loss:

1259

1260

1261

1262

$$\mathcal{L}_{\text{angle}} = \frac{1}{N} \sum_{i=1}^N [(f_{\text{angle}}(h_i^-) - g(h_i^+, h_i^-))^2 + f_{\text{angle}}(h_i^+)^2]$$

1263

1264

Final rotation step:

1265

1266

1267

$$\hat{h} = \frac{\sin(\gamma_1)}{\sin(\gamma_2)} \dot{h} + \frac{\sin(\gamma_2 - \gamma_1)}{\sin(\gamma_2)} h$$

1268

1269

Polarity decision:

1270

1271

$$\hat{\sigma} = \lfloor f_{\text{probe}}(h) \rfloor$$

1272

E DISCUSSION

1273

E.1 SIGNIFICANCE OF SIMS

1274

1275

Model steering versus self-critic RL. Model steering learns lightweight functions that act on intermediate activations of a *frozen* model at inference time. In contrast, self-critic RL optimizes a *trainable* policy via gradient updates on parameters using self-produced preferences or critiques. Practically, steering is plug-in and architecture-agnostic (no weight updates), whereas self-critic RL entails training dynamics (credit assignment, stability/regularization, exploration) and the compute/memory footprint of optimization.

1282

1283

1284

1285

1286

1287

1288

SIMS *versus* **decoding-time value/constraint guidance**. Decoding-time guidance evaluates or scores tokens as they are generated and adjusts next-token probabilities at *every* step, coupling latency to sequence length and the cost of the auxiliary scorer/controller. Sims instead *precomputes* layer-wise steering transforms that shift residual-stream activations during a forward pass. This yields an inference cost that scales with the number of layers via small matrix operations, without per-step scoring or backprop, and keeps memory stable across the decode.

1289

1290

1291

1292

1293

Steering functions versus LoRA. LoRA adapts model *weights* via low-rank trainable matrices learned with backprop; deployment replaces or composes altered weights with the base model. Steering functions leave weights unchanged and operate on *activations* at run time. Consequently, LoRA requires task- or model-specific fine-tuning and checkpoint management, while steering can be learned once from activations and applied to frozen checkpoints with minimal integration overhead.

1294

1295

SIMS *versus* **label-free RL**. (1) *Learning paradigm*. Label-free RL learns or fine-tunes a policy using self-generated preference signals. Sims learns small activation transforms that modulate internal representations at inference, leaving the underlying policy fixed. (2) *Compute/engineering cost*.

1296 Label-free RL entails iterative gradient updates, rollouts, and stability controls; SIMS trains compact
1297 transforms (often linear/affine), then applies them as inexpensive forward operations. (3) *Objective*
1298 *focus*. Label-free RL optimizes a return defined by intrinsic or self-derived rewards, often seeking new
1299 capabilities or strategy shifts. SIMS targets *consistent behavioral alignment* by nudging hidden states
1300 toward desired manifolds and away from undesired ones, prioritizing controllability and efficiency
1301 over learning a new policy from scratch.

1302 The fundamental trade-offs between model steering and alternative solutions are as follows. Model
1303 steering is lightweight, modular, inference-efficient, but may have limited expressiveness. LoRA/self-
1304 critic RL are more expressive but require parameter updates and higher computational costs.
1305

1306 This work represents a paradigm shift from existing model steering approaches. All prior methods
1307 (e.g., ActADD, CAA, HPR) require high-quality, externally annotated preference data (human-labeled
1308 positive/negative examples) that are often costly to obtain, error-prone, and directly constrain their
1309 applicability. SIMS eliminates this critical dependency by generating its own contrastive training
1310 signals through iterative self-evaluation. To realize this supervision-free framework, we develop
1311 several novel techniques: (1) self-generated contrastive sampling that creates training signals from the
1312 model’s own outputs, (2) iterative refinement cycles that progressively improve steering effectiveness,
1313 and (3) prompt ranking and contrast sampling strategies that optimize sample quality without external
1314 guidance.

1315 F USE OF LLM

1316 We used a large language model (LLM) only for language editing (clarity, grammar, and tone). The
1317 LLM did not generate ideas, code, analyses, figures, tables, or experimental results. No proprietary
1318 or sensitive data were shared with the LLM. All mathematical statements, algorithmic descriptions,
1319 citations, and empirical results were written, verified, and are the responsibility of the authors. Model
1320 suggestions were reviewed by the authors for accuracy, and any references were independently
1321 checked. Further details are provided in the paper’s supplementary materials.
1322

1323
1324
1325
1326
1327
1328
1329
1330
1331
1332
1333
1334
1335
1336
1337
1338
1339
1340
1341
1342
1343
1344
1345
1346
1347
1348
1349